

Environmental effects on microstructure and strength of SiC-based hot gas filters

Pirjo Pastila *, Vesa Helanti, Antti-Pekka Nikkilä, Tapio Mäntylä

Institute of Materials Science, Tampere University of Technology, PO Box 589, 33101 Tampere, Finland

Received 23 August 2000; received in revised form 28 November 2000; accepted 9 December 2000

Abstract

The aggressive process environment in advanced coal-fired power generation systems causes microstructural changes in the ceramic hot gas filters used to clean the fuel gas. Changes in microstructure and their effect on strength were studied for commercial SiC-based clay bonded hot gas filters exposed to high temperature, water vapour and gaseous sodium compound. Exposures caused significant crystallization of the binder phase and oxidation of SiC. Loss in strength also occurred. The microstructural changes and their effect on strength are discussed. © 2001 Elsevier Science Ltd. All rights reserved.

Keywords: Filters; Microstructure-final; SiC; SiO₂; Strength

1. Introduction

Ceramic hot gas filters are used in advanced coal-fired power generation systems to clean the fuel gas.^{1,2} Aggressive process environments containing steam, dust, gaseous sulphur and alkali³ cause microstructural changes in all common hot gas filter materials, including oxide, non-oxide and mixed oxide ceramics.^{2,4} These changes — crystallization, oxidation and softening of glassy phases — affect filtration efficiency, long term reliability, strength and creep properties of the filters.^{2,4–8}

In hot gas filtration, the hot (300–900°C), pressurized (10–25 bar) fuel gas from the combustion process is led through ceramic filters.^{2,3} Cleaning of the fuel gas is required to meet the environmental regulations and to prevent corrosion and erosion of turbine blades and other downstream components.^{1,3} Hot gas filters need to operate reliably for more than 10 000 h, maintaining particulate removal efficiencies, high flow capacity and low pressure drop.² They should also possess durability and reliability against mechanical and thermal stresses.²

Silicon carbide (SiC) is a commonly used filter material because of its high temperature strength and thermal shock resistance. A major disadvantage is its

oxidation to silica in high temperature, water vapour environments. Water vapour enhances oxidation of SiC^{9–11} and devitrification of SiO₂ scale.^{12–14} Oxidation of dense SiC is well studied.^{10,12,13,15} Studies are usually made for pure and dense SiC samples and are typically carried out at temperatures higher than 1000°C, since oxidation at lower temperatures is negligible. In hot gas filters SiC grains are bound together with a clay based binder containing alkali and aluminosilicates. Oxidation of silicon carbide in hot gas filters at operation environments below 900°C has been detected in microstructural studies of used filters.^{4,6}

Oxidation and further crystallization of pressureless sintered SiC to cristobalite at 1300°C in water vapour has been concluded to have little effect on the flexural strength of dense samples.¹¹ For porous SiC materials, the effect of oxidation and crystallization on strength may be more significant, since pores enable oxidation throughout the sample, not only on the outer surfaces. SiC-based hot gas filters have been found to lose some of their strength in the filtration process.^{4,5,8}

We exposed several commercial SiC-based hot gas filters at 870°C and atmospheric pressure to water vapour and gaseous sodium containing environments. The exposure environments were selected to simulate real combustion environments. Exposures 1000 h long caused changes in microstructure of the filter body. The changes in strength of the filters were studied.

* Corresponding author.

E-mail address: pirjo.pastila@tut.fi (P. Pastila).

2. Materials and methods

A study was made of five commercial grade SiC-based hot gas filters: Schumacher Dia-Schumalith F 40 (A), Dia-Schumalith 10-20 (B), Pall Vitropore 442T (C), Pall 326 (H), and Dia-Schumalith T F 20 (I). Filters typically contained 200 μm SiC grains bonded with a clay based silicate binder (Fig. 1). The overall porosity was roughly 40%. Four laboratory exposures at 870°C and atmospheric pressure 1000 h long were made for tubular samples 40 cm in length cut from the filters. The environments of the exposures described in Table 1 were selected to simulate real combustion environments. In exposure 1 the environment was uneven since the test chamber was damaged during the exposure. In exposure 3 SO₂ gas reduced the sodium oxide concentration to less than one hundredth of that in exposure 2. In exposure 4 the filter surfaces were coated with coal ash. The ash contained 0.7 wt.% sodium. Filters B and C were tested in exposures 1 and 2; filter I in exposures 3 and 4; filter H in exposures 2, 3 and 4; and filter A in all four exposures.

Microstructural characterization of the filters was done by X-ray fluorescence (XRF), flame atomic adsorption spectroscopy and solid-state infrared adsorption

methods for chemical composition, X-ray diffraction (XRD) for phase detection, and scanning electron microscopy (SEM) for microstructural details. Rautaruukki Research Center of Rautaruukki Steel made the chemical analyses. The amount of binder was calculated from chemical analyses assuming that carbon is present only as SiC. All other elements were assumed to be in oxide form in the binder. Both quantitative and qualitative XRD analyses were carried out. Quantitative analysis using an internal standard method¹⁶ was made for crushed and sieved (0.09 mm) samples. The sources of error in the quantitative analysis are overlapping of the peaks, small amounts of other phases than SiC in the samples, and the fact that samples used to determine the calibration curve of single phase may slightly differ from phases in actual samples. XRF results were used together with XRD results to estimate the composition of the binder of the filters. SEM investigation was made for HF-etched and non-etched cross-sections. Samples were simply cut with a precision cutter then etched and mounted to the sample holder. All SEM samples were gold coated.

Strength testing was done at room temperature by the internal hydraulic pressure (IHP) method.¹⁷ Ring-shaped specimens cut from the filters were loaded internally by hydraulic pressure. Nominal dimensions of the specimens were 60 mm outer diameter, 10 mm wall thickness and 20 mm width. The numbers of tested specimens are given with the results. Strength was calculated from the maximum pressure detected. Results were analysed following the standard ENV 843-5.

3. Results

3.1. Microstructural characterization

The primary differences in the unexposed filters were the amount of crystalline phases in the binder and the composition of the binder. In filters A and B it contained more than 70% amorphous phase. In filter C the binder contained the largest amount of alkalis and was almost totally amorphous, Fig. 1. The binder of filter I was clearly crystalline in nature but contained some amorphous phase. The binder of filter H was mainly crystalline (Fig. 1), but areas of amorphous alkali silicates were found in thick layers of the binder between the SiC grains. According to XRD, the crystalline phases in the binders of unexposed filters were cristobalite, mullite and alkaline aluminosilicates like albite. A layer of cristobalite crystals on the surface of SiC was found in unexposed filters A, B, H and I. The thickness of the crystal layer was 1 μm in filters A and B and 2–3 μm in H and I.

The exposures caused changes in the amount and composition of the binder. The amounts of the binder

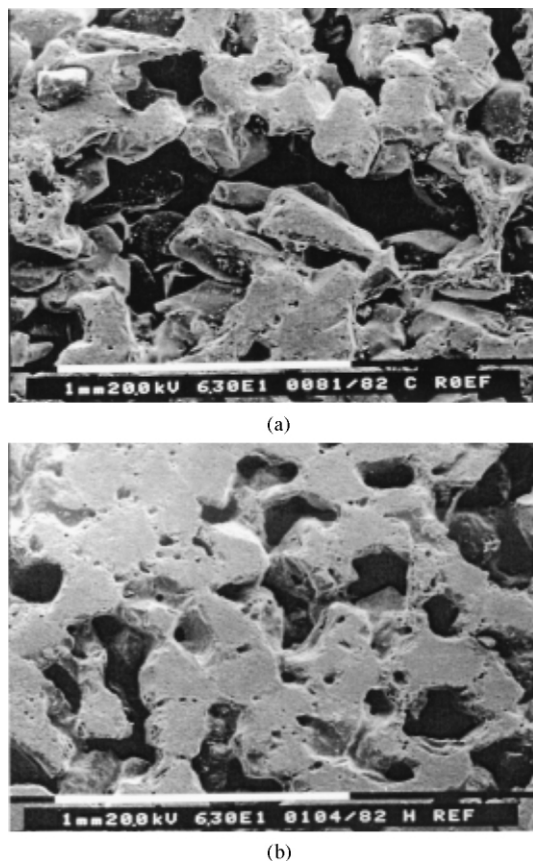


Fig. 1. Typical cross sections of unexposed SiC-based clay bonded hot gas filters. (a) Binder of filter C was almost totally amorphous. (b) Binder of filter H was almost totally crystalline.

Table 1
Exposure environments

Exposure	Total gas flow (l/min)	Air (l/min)	CO ₂ (l/min)	SO ₂ (ppm)	H ₂ O(g) (l/min)	Na ₂ O	Other
Exp. 1	7	6	0.5	0	0.5	~100 ^a	
Exp. 2	30	18–20	0.7–1	0	10	15–20 ^b	
Exp. 3	30	25–27	0.8–1.3	200	2–2.5	0.1 ^b	
Exp. 4	30	25–27	0.8–1.3	200	2–2.5	~0 ^c	Ash ^d

^a Sodium carbonate dissolved to water was sprayed into chamber. Consumed sodium carbonate suggests 100 ppm Na₂O concentration. The failure of the test chamber caused uneven and localised exposure.

^b Sodium oxide concentration calculated assuming thermal equilibrium. In exposure 2 was sodium as sodium hydroxide and in exposure 3 as sodium sulphate. In exposures 2 and 3, sodium source was inside the test chamber near the incoming gas inlet.

^c In exposure 4 there was no other sodium source than the ash on the filter surfaces.

^d Filters were coated with coal ash before being placed in the test chamber. Foster Wheeler Energia Oy delivered the ash.

according to chemical analyses of the filters are presented in Table 2. The amount of binder was calculated from the chemical composition assuming that carbon is present only as SiC. The increases in the amount of binder that occurred especially clearly in filters A and I in exposure 4, could only be explained by oxidation of SiC grains. Because of the way the amount of binder was calculated, the increase in the amount of binder means decrease in the amount of SiC in the filter. The main chemical components of the binder in all filters were silica and alumina. Changes in the binder compositions due to exposures were in general small. Alkali concentrations both increased and decreased in a varying way from filter to filter. The increase in the amount of binder due to oxidation of SiC apparently decreased alkali concentrations.

The major phases identified by XRD were SiC, cristobalite, mullite and albite. The exposures caused increase in the amount of cristobalite as shown in Table 2. Formation of cristobalite in exposures was most clearly seen in filter A, but it occurred in all filters. Fig. 2 presents diffractograms of samples from filter A in unexposed and exposed conditions. Both low temperature α - and high temperature β -cristobalite were found at room temperature from exposed filters. Ca²⁺ or Al³⁺-ions in the cristobalite can prevent the α - β transformation.¹⁸ From unexposed filters we found only α -cristobalite. Also Oakey et al.⁸ found β -cristobalite in filters similar to filter A, operated in a pressurized fluidized bed combustor at Grimethorpe, UK. Aside from increasing the intensity of cristobalite, crystallization of the binder was shown as the appearance of albite and possibly other alkaline aluminosilicates in the diffractograms. Their precise identification was impossible since these silicates have complex crystal structures and give rise to many peaks that are overlapping or close to each other. Distorted structures causing shift of the peaks are also possible.

The effect of the exposures was most clearly shown by SEM investigation. Typical microstructures of the unexposed filters are shown in Figs. 3–5. During the exposures, the outer surfaces of the binder were crystal-

Table 2
Amount of binder and relative cristobalite content of the crystalline binder phases in filters^a

Filter	Unexposed	Exposure 1	Exposure 2	Exposure 3	Exposure 4
Filter A					
Binder wt.% ^a	17.7	— ^d	16.3	— ^d	25.5
Cristobalite % ^b	100%	680%	492%	459%	608%
Filter B					
Binder wt.%	14.7	24.8	19.3	*	*
Cristobalite %	100%	185%	182%	*	*
Filter C					
Binder wt.%	17.2	20.1	17.3	*	*
Cristobalite %	100%	768%	450%	*	*
Filter H					
Binder wt.%	27.5	* ^c	26.6	28.1	29.1
Cristobalite %	100%	*	83%	105%	107%
Filter I					
Binder wt.%	19.8	*	*	21.9	28.6
Cristobalite %	100%	*	*	156%	180%

^a The amount of binder is calculated from the chemical composition assuming that carbon is present only as SiC. Values are given in wt.%.

^b The amount of cristobalite by the quantitative XRD analysis was taken to be 100% in unexposed filter.

^c *Filter was not in the exposure.

^d No data available.

lized and the layer of cristobalite on SiC surfaces was increased in thickness. There was no consistent difference in the effects of exposures on microstructures. All exposures of filter A caused crystallization of outer surfaces of the binder (Fig. 3), similar crystallization occurred in filters B and C. The cristobalite layer on the SiC grains of filters A and B grew in thickness (Fig. 3). There was no cristobalite layer on the SiC grains of filter C when unexposed or after exposure 2. Only after exposure 1 small crystals, less than 1 μ m in size were found between SiC and the binder. Despite the significant crystallization in the exposures, the binder in filters A, B and C remained mainly amorphous. In places where there was less binder between the SiC grains,

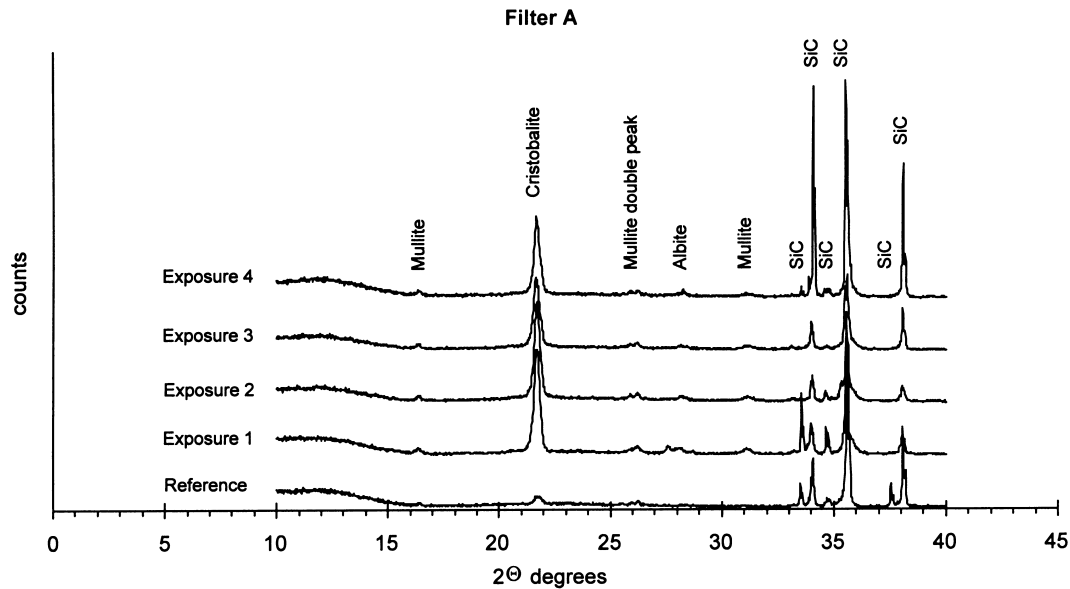


Fig. 2. Diffractograms of samples from filter A as unexposed (reference) and after different exposures.

areas of throughout crystallized binder were sometimes found. Though the binder in filters H and I contained only a few amorphous areas, exposures caused crystallization in these filters too. In filter H crystallization of amorphous areas on the outer surface of the binder led to cracking in the binder (Fig. 4). In filter I, the cristobalite layer on the SiC surface grew in size. The outer surfaces of the binder became totally crystallized (Fig. 5). An amorphous layer, less than 100 nm thick, was formed between cristobalite and SiC in filter I exposure 3 (Fig. 6). This layer was more resistant against HF etching than the amorphous phase of the binder above the cristobalite grains. This difference in resistance to HF suggests that the layer was pure SiO_2 . Since the total amount of binder phase increased by 2 wt.% in exposure 3 (Table 2), the amorphous layer must be due to oxidation of SiC.

3.2. Strength

The median strength, unbiased estimate of Weibull modulus with 0.9 confidence interval and the number of samples tested are given in Table 3. Strength of the filters decreased due to the exposures, as expected. The reduction in strength, both absolutely and relatively, was least for filter I. For the other filters the decrease was roughly 30%. Before exposure filter B had the best median strength and Weibull modulus. Strength data for filter B after exposures 1 and 2 are not available, but the same kind of strength reduction can be assumed as for filters A, C and H. Decreases in Weibull modulus with exposure occurred for all filters except filter A (Table 3). Despite the small number of samples, the 0.9 confidence intervals of the unbiased Weibull modulus do not overlap significantly. This indicates an increase

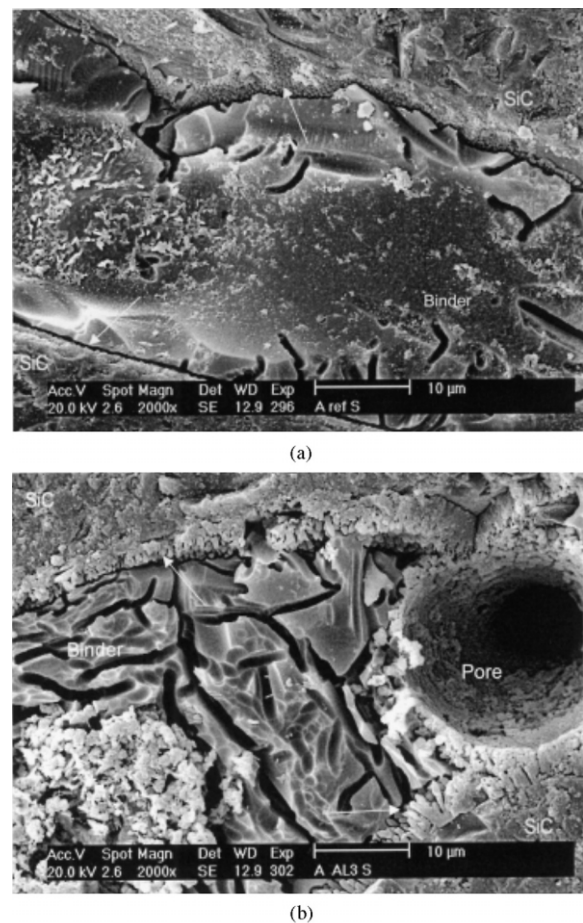
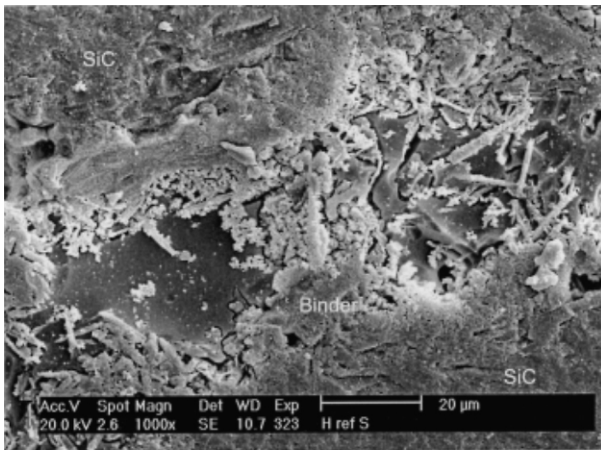
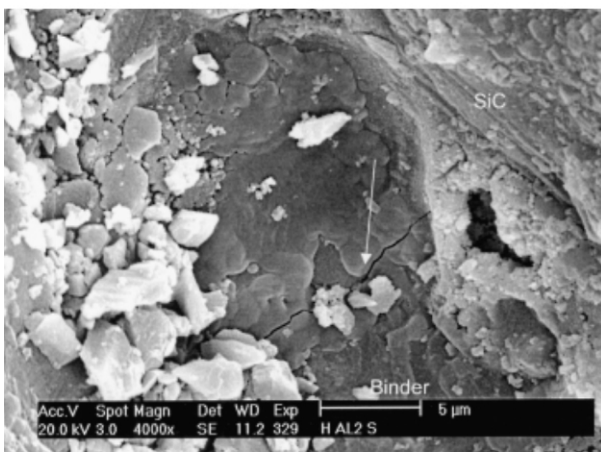


Fig. 3. Binder between SiC grains in filter A. HF-etched diamond saw cut cross sections. (a) Amorphous aluminosilicate binder between two SiC grains in the unexposed filter. Note the crystals on the SiC grains pointed with arrows. (b) Exposure 3 caused crystallization on the outer surfaces of the binder and the crystals on SiC grew in size.



(a)



(b)

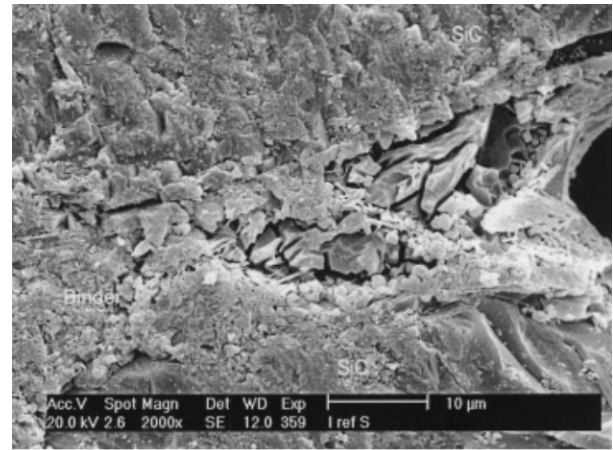
Fig. 4. Binder in filter H. HF-etched diamond saw cut cross sections. (a) A glassy area in the binder of unexposed filter. (b) A microcrack found after exposure 2 from the originally glassy binder area.

in the critical flaw size distribution due to microstructural changes in exposures. That is, the filters became more unreliable. The increase of Weibull modulus for filter A indicates the formation of a fairly uniform flaw population that specifies the strength of filter A.

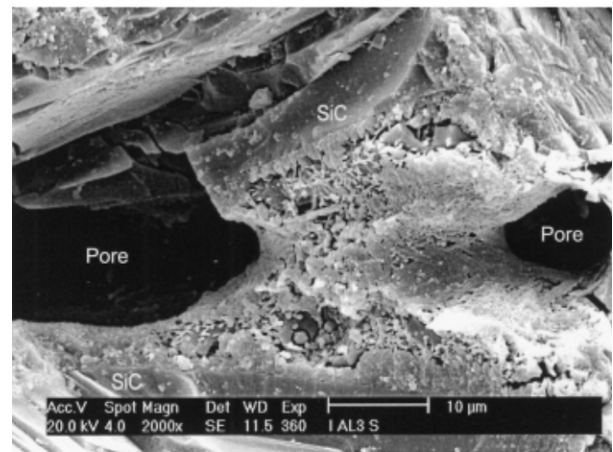
4. Discussion

The main effects of the exposures on filters were oxidation of SiC, crystallization of the binder and decrease in strength. All these changes have been described for filters used from several hundreds to thousands of hours in coal combustion environments.^{4,6,8}

Water vapour is a more severe oxidizer than oxygen for SiC. Furthermore, it has been shown that, in the presence of water vapour, sodium enhances the oxidation of SiC.^{10,19} Water vapour is capable of diffusing through an alkaline silicate binder²⁰ and the presence of alkaline silicates next to SiC provides necessary impurities. Considering the long exposure time (1000 h) in



(a)



(b)

Fig. 5. Binder between SiC grains in filter I. HF-etched diamond saw cut cross-sections. (a) As unexposed, (b) after exposure 3. Outer surface of the binder crystallized in the exposure.

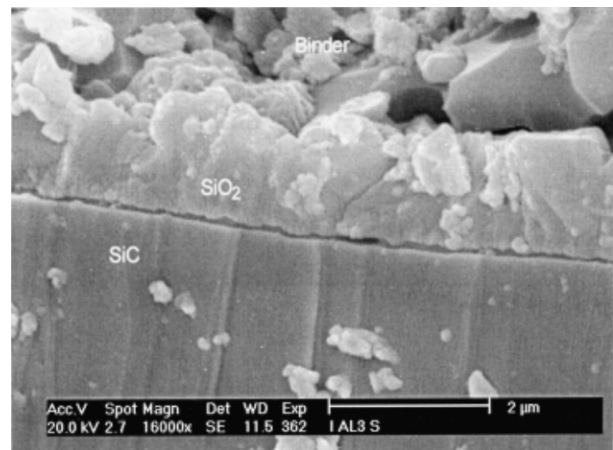


Fig. 6. An amorphous layer between SiC and cristobalite crystals found from filter I after exposure 3. HF-etched diamond saw cut cross-section.

water vapour and sodium containing environment, oxidation of SiC may reasonably occur. Devitrification encourages further oxidation of SiC.¹¹

Results of Opila¹⁰ and Maeda et al.¹¹ show increasing oxidation of dense and pure SiC with increasing water vapour content. However, according to our results, exposure 2 with the highest vapour content, caused only negligible increase in the amount of binder in filters A, C and H. We did not find a correlation between the content of water vapour or sodium oxide in the exposure environments and the amount or alkali concentration of the binder. This suggests that water vapour is a necessary but not sufficient factor for the oxidation of SiC-based hot gas filters at 870°C. The amount of cristobalite (Table 2) increased in all exposed filters except in filter H in exposure 2. All filters except filter C had an initial cristobalite layer on SiC grains which grew in thickness in the exposures. We believe this growth to be mainly a result of SiC oxidation to SiO₂ and successive crystallization. Oakey et al.⁸ stated that this growth of cristobalite occurred by devitrification from the binder. In this case there should have been an amorphous layer between the cristobalite and SiC due to oxidation of SiC. This was detected only for filter I in exposure 3. Devitrification of SiO₂ from binder to cristobalite also occurred in the silica rich areas, especially on the pore sides. Water vapour and low concentrations of sodium facilitate crystallization of SiO₂ to cristobalite.^{12,14} According to Opila,¹⁰ it is impurities rather than water

vapour that enhance the nucleation rate of cristobalite. In the present study both factors were operative.

Oxidation of SiC to silica causes volume expansion of the material up to 100%. Further crystallization of silica to cristobalite may cause tensile stresses or cracks in the cristobalite layer since cristobalite is of lower volume than amorphous silica. Displacive α - β phase transformation of cristobalite at 200–270°C causes 3% change in volume. Thermal expansion coefficients are significantly different for SiC, cristobalite and amorphous silica.¹² Differences in the thermal expansion coefficients may cause tensile stresses and cracking of the oxide scale.¹² This has been observed for silica samples in corrosion tests in oxidizing atmospheres with aqueous Na₂SO₃.¹⁴ All exposed filters decreased in strength. In the exposed filters, crystallization of SiO₂ induced microcracks that became stress concentrators, especially on the side of pores. Volume changes and thermal expansion mismatches upon cooling after exposure may have caused local stresses. Local stresses combined with microcracks caused severe stress concentrations, which was macroscopically seen as decrease in the strength of exposed filters. Since the strength testing was made at room temperature the primary source of cracking is most probably the cristobalite α -> β transform. It is likely that the strength decrease is less if the filters which are continuously used at operation temperature. However, interruptions in service cause cooling through cristobalite phase transition temperature.

Table 3
Median strength, unbiased Weibull modulus, 0.9 confidence interval for Weibull modulus estimate and number of samples tested

Filter	Unexposed	Exposure 1	Exposure 2	Exposure 3	Exposure 4
Filter A					
Median strength MPa	19.8	13.7	13.5	13.8	16.7
Weibull modulus	15 [11–22] ^c	52 [27–108]	22 [13–40]	26 [15–51]	27 [19–41]
No of specimens	18	5	7	6	13
Filter B					
Median strength MPa	34.5	– ^b	–	* ^a	*
Weibull modulus	29 [22–40]	–	–	*	*
No of specimens	20				
Filter C					
Median strength MPa	19.7	–	13.7	*	*
Weibull modulus	33 [24–46]	–	13 [7–28]	*	*
No of specimens	18		5		
Filter H					
Median strength MPa	27.6	*	17.3	20	19.9
Weibull modulus	27 [19–40]	*	21 [11–46]	15 [8–29]	15 [8–33]
No of specimens	13		5	6	5
Filter I					
Median strength MPa	15.5	*	*	14.6	15.8
Weibull modulus	33 [23–47]	*	*	12 [6–26]	7 [4–17]
No of specimens	15			5	5

^a * Filter was not in the exposure.

^b –No data available.

^c [. . .] 0.9 confidence interval of biased Weibull modulus estimate.

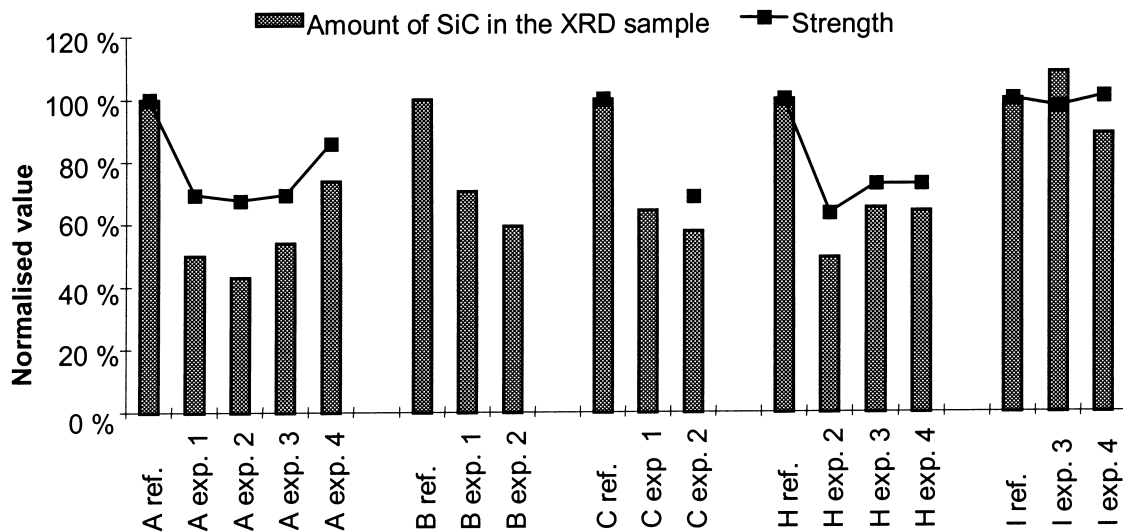


Fig. 7. Amount of SiC in crushed and sieved XRD sample and measured strength of filters. Unexposed samples are used as reference. All values are normalised with appropriate reference value.

We found a correlation between strength of the filters we tested and amount of SiC in the crushed and sieved XRD sample (Fig. 7). The higher the strength the more SiC was in the sample. The binder or the bond between binder and SiC grain was weaker in exposed than in unexposed filters with one exception of filter I in exposure 3. In filter I in exposure 3 there was more SiC in the exposed than unexposed XRD sample but the strength was lower in the exposed than unexposed samples. Oakey et al.⁸ report a change in the fracture mode of filters similar to filter A used at Grimethorpe. In the as-received filters, the fracture path was mainly through the SiC grains. In the filters used at the Grimethorpe combustor, the fracture path was mainly through the binder. This change was suggested to occur because the crystallization caused microcracking at the interface of SiC and binder. The weakening of the bond between SiC grain and binder reported by Oakey et al.⁸ could explain the increase in the Weibull modulus for filter A when exposed. However, in the other exposed filters Weibull modulus decreased, which suggests the microcracking of the binder on the pore sides to be important.

5. Conclusions

Exposures of commercial SiC-based clay bonded hot gas filters to water vapour and gaseous sodium at 870°C and atmospheric pressure cause oxidation of SiC grains and crystallization in the binder. These microstructural changes decrease the strength of filter markedly. In real operation conditions, mechanical and thermal stresses combined with microstructural changes may cause continuous degradation of strength and finally failure of the filter. To predict, how long is the safe service time of

filters, more detailed oxidation studies and a fracture mechanical approach are needed.

Acknowledgements

The authors wish to acknowledge TEKES Technology Development Centre, Ensto Ceramics Oy, Fortum Power and Heat Oy and Foster Wheeler Energia Oy for cooperation and financial support.

References

1. Stringer, J. and Leitch, A. J., Ceramic candle filter performance at the Grimethorpe (UK) pressurized fluidized bed combustor. *J. Eng. Gas Turbine Power-T ASME*, 1992, **114**, 371–378.
2. Alvin, M. A., Lippert, T. E. and Lane, J. E., Assessment of porous ceramic materials for hot gas filtration applications. *Am. Ceram. Soc. Bull.*, 1991, **70**, 1491–1498.
3. Oakey, J. E. and Fantom, I. R., Hot gas cleaning — materials and performance. *Materials at High Temperatures*, 1997, **14**, 337–345.
4. Alvin, M. A., Performance and stability of porous ceramic candle filters during PFBC operation. *Materials at High Temperatures*, 1997, **14**, 355–364.
5. Spain, J. D. and Starrett, H. S., Characterization of monolithic and composite filter elements. In *High Temperature Gas Cleaning Volume II*, ed. A. Dittler, G. Hemmer and G. Kasper. Institut für Mechanische Verfahrenstechnik und Mechanik der Universität Karlsruhe (TH), Karlsruhe, 1999, pp. 414–427.
6. Alvin, M. A., Hot gas filter development and performance. In *High Temperature Gas Cleaning Volume II*, ed. A. Dittler, G. Hemmer and G. Kasper. Institut für Mechanische Verfahrenstechnik und Mechanik der Universität Karlsruhe (TH), Karlsruhe, 1999, pp. 455–467.
7. Pastila, P. H., Nikkilä, A.-P. and Mäntylä, T. A., The effect of oxidation on creep of clay bound SiC filters. *Ceram. Eng. Soc. Proc.*, 1998, **19**, 37–44.

8. Oakey, J. E., Lowe, T., Morrell, R., Byrne, W. P., Brown, R. and Stringer, J., Grimethorpe filter element performance — the final analysis. *Materials at High Temperatures*, 1997, **14**, 371–381.
9. Jorgensen, P. J., Wadsworth, M. E. and Cutler, I. B., Effects of water vapour on oxidation of silicon carbide. *J. Am. Ceram. Soc.*, 1961, **44**, 258–261.
10. Opila, E. J., Variation of oxidation rate of silicon carbide with water-vapour pressure. *J. Am. Ceram. Soc.*, 1999, **82**, 625–636.
11. Maeda, M., Nakamura, K. and Ohkubo, T., Oxidation of silicon carbide in a wet atmosphere. *J. Mat. Sci.*, 1988, **23**, 3933–3938.
12. Jacobson, N. S., Corrosion of silicon-based ceramics in combustion environments. *J. Am. Ceram. Soc.*, 1993, **76**, 3–28.
13. Fergus, J. W. and Worrell, W. L., The oxidation of chemically vapour deposited silicon carbide. In *Ceramic Transactions Vol. 10, Corrosion and Corrosive Degradation of Ceramics*, ed. R. E. Tressler and M. McNallan. American Ceramic Society, Westerville, OH, 1990, pp. 43–51.
14. Lawson, M. G., Kim, H. R., Pettit, F. S. and Blachere, J. R., Hot corrosion of silica. *J. Am. Ceram. Soc.*, 1990, **73**, 989–995.
15. Zheng, Z., Tressler, R. E. and Spear, K. E., Oxidation of single-crystal silicon carbide. *J. Electrochem. Soc.*, 1990, **137**, 2812–2816.
16. Cullity, B. D., *Elements of X-ray Diffraction*, 2nd edn. Addison-Wesley, USA, 1978, pp.415-420.
17. Helanti, V., Mäntylä, T., Isaksson, J., Eriksson, T. and Ståhlberg, P., Strength testing of tubular ceramic gas filters by internal hydraulic pressure test. In *Proceedings of the Second International Conference on “Ceramics in Energy Applications”*. The Institute of Energy, London, 1994, pp. 331-337.
18. Salzberg, M., Bors, S., Bergna, H. and Winchester, S., Synthesis of chemically stabilized cristobalite. *J. Am. Ceram. Soc.*, 1992, **75**, 89–95.
19. Ervin, G. Jr., Oxidation behaviour of silicon carbide. *J. Am. Ceram. Soc.*, 1958, **41**, 347–352.
20. Schlichting, J., Oxygen transport through silica surface layers on silicon-containing ceramic materials. *High Temperatures — High Pressures*, 1982, **14**, 717–724.